

# Modeling the human cardiovascular system with a special focus on the heart using Dymola

Stefanie Heinke, Carina Pereira, Jan Spillner, and Steffen Leonhardt.

**Abstract**—Severe heart failure is a common problem that has a significant effect on health expenditures in industrialized countries; moreover it reduces patient's quality of life. However, current research usually focuses either on detailed modeling of the heart or on detailed modeling of the cardiovascular system. Thus, this paper aims to present a sophisticated model of the heart enhanced with an extensive model of the cardiovascular system. Special interest is on the pressure and flow values close to the heart since these values are critical to accurately diagnose causes of heart failure. The model is implemented in Dymola an object-oriented, physical modeling language. Results achieved with the novel model show overall feasibility of the approach. Moreover, results are illustrated and compared to other models. The novel model shows significant improvements.

**Keywords**—Cardiovascular system, Heart, Modeling.

## I. INTRODUCTION

**C**ARDIOVASCULAR disease is the biggest health problem in industrialized countries. In many cases, patients suffer from heart attack or dilated cardiomyopathy leading to an insufficient cardiac output, also called heart failure. The consequence is an inappropriate perfusion of the human body associated with under-supply of nutrients and oxygenation.

Presumably due to the historical development, research focuses either on detailed modeling of the cardiovascular system or on detailed modeling of the heart. However, only detailed models of the cardiovascular system have the ability to mimic pulse wave reflections especially resulting from impedance changes in the arterial vascular system. Since the characteristics of these pulse wave reflections have a significant impact on the heart and other organs, physicians are advised to consider these to find the best therapy for a patient (see[1]). In addition, these models can simulate the distribution of the cardiac output to distinct organs.

Models of the native heart, on the other hand, allow simulation of various diseases of the heart like heart failure. Moreover, since some heart models contain the septum, they can even mimic the pressure volume relationship between the ventricles yet, they do not incorporate reflections resulting from the vascular system.

Hence, this paper aims to present a detailed heart model embedded into a detailed model of the cardiovascular system. Therewith, it is possible to simulate heart or vascular diseases

and to analyze their interactions as well. Such a model might also be a valuable tool towards understanding the interactions of a mechanical blood pump like a ventricular assist device (VAD) or total artificial heart (TAH) with the complete cardiovascular system. Since these devices are connected to the atria, ventricles, pulmonary artery or aorta ascendens it is crucial to accurately simulate the pressures at the inlets and the outlets of such a pump.

The following model description is splitted into four sections. At the beginning the cardiovascular model by Leaning et al. [2] is briefly presented, since the cardiovascular part of the model is based on this paper. In the following the heart model provided by Smith et al. [3], [4] is introduced, which is the basis for the heart model. Afterwards, extensions and adaptations in the models are discussed. The models are implemented in Modelica®, an object-oriented modeling language that represents the modular structure of the model. Therefore, in the fourth part a short introduction into Dymola is also given.

## II. METHODS

### A. Model of the human cardiovascular system

The implemented cardiovascular model goes back to the proposed model by Leaning et al. [2] and Beneken and deWit [5]. It simulates the hydrodynamic behaviour of the cardiovascular system using lumped parameters. In its basic version, the model consists of 19-segments as presented in Fig. 1. The heart model is given by four chambers, left and right atrium and left and right ventricle. Each of them is activated via a sine function  $e_L(t)$ , where the index "L" stands for "Leaning". The pressure-volume relationship of the chambers is given by:

$$p(t) = e_L(t) \cdot (V(t) - V_u), \quad (1)$$

where  $p(t)$  is the pressure inside a chamber,  $V_u$  is a parameter for the unstressed volume of the chamber and  $V(t)$  is the variable volume of the chamber. Tricuspid and mitral valve are represented by diodes having only a small pressure drop across them. The aortic and pulmonary valve also incorporate an inrtance effect.

The lung consists of the pulmonary artery and vein, which both differ slightly from the artery and vein model used in the rest of the vascular system to account for the critical closing pressure in the lung. All bigger arteries (indicated by the solid line (—)) are represented by a combination of a resistance R, inrtance L and a capacitance C as shown in the enframed box in Fig. 1. For the veins (shown by dash-dot lines (— · —)) extended with diodes), RC-models are

S. Heinke and S. Leonhardt are with the Philips Chair for Medical Information Technology, RWTH Aachen University 52074 Aachen, Germany (see <http://www.medit.hia.rwth-aachen.de/go/id/tgw/?lang=en>).

C. Pereira is a graduate student of the Department of Industrial Electronics, University of Minho, 4800-058 Guimares, Portugal.

J. Spillner is with the the department of cardiac and thorax surgery, University Hospital Aachen, 52074 Aachen, Germany

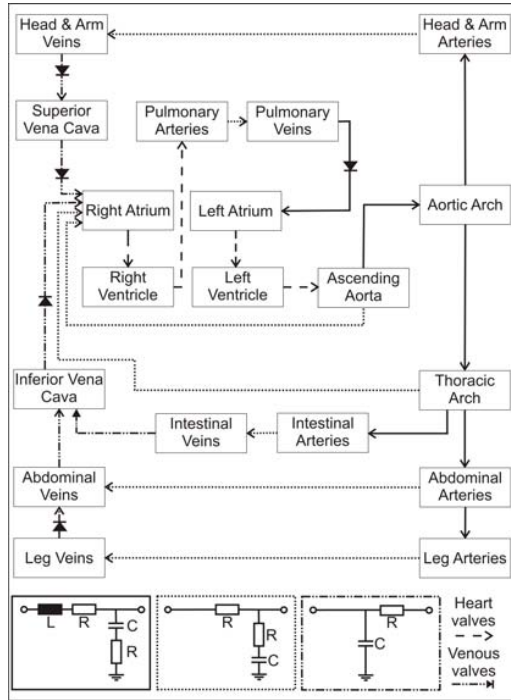


Fig. 1. Overview on the cardiovascular model, modified from [2]

used. The diodes illustrate the behaviour of the venous valves, which allow only little reflux in the veins. Segments that are connected via dotted lines ( $\cdots$ ) are interpreted as arteries, too. Since these are smaller arteries, the inertance effect of the blood is neglected. The blood flowing from the ascending aorta to the right atrium is considered to be the coronary flow.

In its complete version, the original model from [2] also contains the arterial baroreceptor reflex. The arterial baroreceptor reflex has been implemented but is not discussed in this paper.

### B. Model of the human heart

The implemented heart model is based on publications by Smith et al. [3], [4]. It consists of two active elastic chambers, the left and right ventricle, but it contains the pericardium and the septum as well. Hence, it is possible to simulate the ventricular interaction.

The systemic and the pulmonary circulation are realized in the same way, i.e. the systemic circulation is basically represented by the aorta and the vena cava. They are connected by a resistance according to Poiseuille's law. This concept is also applied to the pulmonary circulation consisting of the pulmonary artery and vein. Aorta, vena cava, pulmonary artery and veins are modelled as passive elastic chambers. Between the ventricles and each of the before mentioned vessels, a flow section was implemented consisting of a diode, a resistance and an inertance. These elements account for the valves at the inlet and outlet of the ventricle, the pressure drop across a section and the inertia of the blood. A detailed section around a ventricle is shown in Fig. 2.

The activation function of the ventricle in this model is derived from the PV-diagram. Hence, first of all the end-systolic and the end-diastolic pressure-volume relationships (ESPVR, EDPVR) are defined:

$$P_{es}(V) = E_{es} \cdot (V - V_u) \quad (2)$$

$$P_{ed}(V) = P_0 \cdot (e^{\lambda \cdot (V - V_0)} - 1). \quad (3)$$

In (2) and (3),  $P_{es}$  represents the end-systolic and  $P_{ed}$  the end-diastolic pressure.  $E_{es}$  stands for the elastance of the end-systolic curve, whereas  $P_0$  in (3) is the elastance of the end-diastolic-curve. The volume  $V_u$  in (2) is the unstressed volume of the ESPVR and  $V_0$  in (3) is the volume at zero pressure of the EDPVR. The curvature of the EDPVR is determined by  $\lambda$ . Equations (2) and (3) define the upper and lower bound for the elastance of the cardiac muscle. In combination the equations lead to (4) describing the pressure  $p(t, V)$  of a chamber:

$$p(t, V) = e_S(t) \cdot P_{es}(V) + (1 - e_S(t)) \cdot P_{ed}(V), \quad (4)$$

$$e_S(t) = e^{-80 \cdot (t - 0.27)^2}, \quad (5)$$

where  $e_S(t)$  is the activation function of the model by Smith et al. [3], [4]. In order to include the ventricular interaction, additional pressure-volume relationships are needed. These volumes do not present the volumes inside a ventricle or a chamber, but the volumes of the cardiac walls. Accordingly, the activation function generates a wall tension in the cardiac walls and with it a pressure. New volumes are introduced for the left and right ventricle (left / right ventricle free wall,  $V_{lvf} / V_{rvf}$ ), the septum ( $V_{spt}$ ) and the pericardium ( $V_{pcd}$ ). In the following, the equations for these volumes are given:

$$V_{lvf} = V_{LV} - V_{spt} \quad (6)$$

$$V_{rvf} = V_{RV} + V_{spt} \quad (7)$$

$$V_{pcd} = V_{LV} + V_{rv} = V_{lvf} + V_{rvf}. \quad (8)$$

Since the heart walls are responsible for the contraction and relaxation of the heart, additional pressure functions for the free walls and the pericardium are defined similar to (4). The pressure for the septum is given by:

$$P_{spt} = P_{lv} - P_{rv} = P_{lvf} - P_{rvf}. \quad (9)$$

### C. Developing a new cardiovascular model

Since TAHs are typically connected to the atria, the heart model presented in section II-B was expanded by two more chambers to account for their behaviour. For consistency purposes, the same activation function for the atria was applied as well as for the ventricles. Except for the offset shift, this activation function was introduced by [6] earlier. The function can be described as follows:

$$e_N(t) = \sum_{i=1}^4 A_i \cdot e^{-\frac{1}{2} \cdot (t - \frac{C_i}{B_i})^2} + D_i. \quad (10)$$

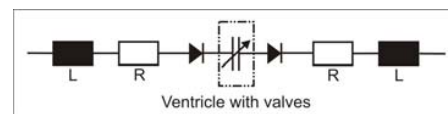


Fig. 2. Flow sections around a ventricle, modified from [4]

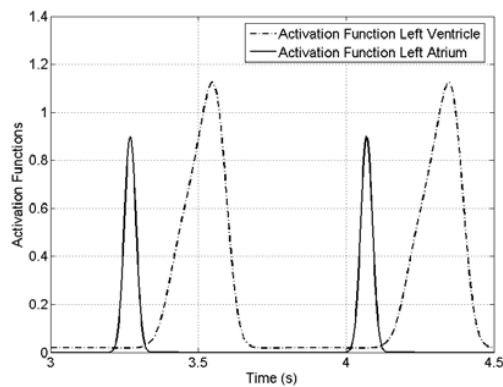


Fig. 3. Activation Function of the left atrium and ventricle

$A_i$ ,  $B_i$  and  $C_i$ ,  $D_i$  are fixed parameters, where  $A_i$  influences the magnitude,  $B_i$  influences the width,  $C_i$  determines the delay of the curve and  $D_i$  is an offset. From this equation the pressure in the chambers can be calculated according to (4). Hence, the activation function for the four chambers results from four gaussian functions. The function is similar to (5). The parameters for the atria were adopted to achieve realistic values. The offset shift is necessary to avoid negative pressures in the left ventricle (compare [7]). Therefore, the trend of the curve (10) and thus the parameters  $A_i$ ,  $B_i$  and  $C_i$  must be adapted. The contraction sequence of the four chambers corresponds to the timing published by [2] assuming an initial heart frequency of 80 bpm. This results in a delay time of ca. 0.27 s for the right ventricle and ca. 0.2 s for the left ventricle compared to right and left atrium as can be seen in Fig. 3 for the left chambers. Additionally, the unstressed volumes in the atria and ventricles were increased as was done for the resistances of the pulmonary and tricuspid valve. In contrast, the resistances of the mitral and the aortic valve were slightly decreased. In a first step this extended heart model was embedded into the cardiovascular model presented in section II-A.

However, in the basic model of the cardiovascular system (see Fig. 1) the head and the arms are combined meaning they are represented by one part of the vascular system. As is known, the brain comes with an autoregulation-mechanism to stabilize its perfusion in a wide range of blood pressures. Therefore, this combination of head and arms is not a valid solution when a model should also be deployed to simulate dynamic exercise in the long-run. Consequently, the vascular system of the arms and the head was detached. In addition, upper-body exercise (arms) has a lower mechanical efficiency than lower-body exercise (legs) [8]. Therefore, the arms were not joined with the vascular system of the legs to a compartment "exercising muscles".

The circuitry of the upper-body part is depicted in Fig. 4. Due to this adjustment in upper-body part of the model the impedance values of each part of the vascular systems were recalculated. Moreover, the resistances as well as compliance values were adapted to match the distribution of the cardiac

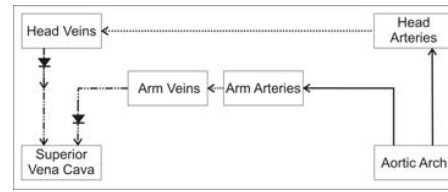


Fig. 4. Upper-body part of extended cardiovascular system model

output to values reported in literature [8], [9], [10]. In particular, values of the small arteries were modified since they have a strong effect on the overall resistance and the distribution of flow. The heart was connected to the model of the arterial baroreceptor reflex to enable autonomous adaption of heart rate and contractility.

#### D. Dymola: A physical, object-oriented simulation language

For the modeling and simulation of the cardiovascular and heart model, Dymola was used. Dymola is a program which is based on the object-oriented modeling language Modelica®. Hence, it permits inheritance of classes. This allows e.g. the definition of a class arteries which can be used several times in the cardiovascular model.

Furthermore, Dymola is a physical modeling language. It is based on Kirchhoff's laws (see [11]). This is a great advantage for modeling the human cardiovascular systems since this allows reverse flows and therefore reactions between components. This means, it allows bidirectional signal flows rather than defining flow directions for each component. This functionality is realized by so called "connectors", which are defined for the components. Connectors are the connection to the outside world of a component. They always consist of at least two variables: a flow and a potential variable. This concept in contrast to a component of Matlab®/ Simulink® is indicated in Fig. 5. Typically a "partial model" that realizes the physical relationship of the connectors of a component is defined as:

```
0=cnProximal.fl+cnDistal.fl;
p_jk=cnProximal.press-cnDistal.press;
fl_jk=cnProximal.fl;
```

In this example the two connectors are called "cnProximal" and "cnDistal", the pressure drop across a component is defined as " $p_{jk}$ " and the flow through a component is given as " $fl_{jk}$ ", "fl" stand for flow and "press" for pressure. This "partial model" is used e.g. for resistances. When defined this way flows into a component are positive, whereas flows out of a component are negative. Naming connectors "cnProximal" and "cnDistal" simplifies the analysis of the results due to defining the expected flow direction. However, the flow direction only depends on the potential difference which is applied to a component. Furthermore, Dymola comes with several integration algorithms. For the simulation of the model proposed by Leaning et al. [2] the standard integration algorithm of Dymola ("dassl") was used, but a few other integration algorithms also performed with this model. However, for the heart model described in section II-B as well as for the new

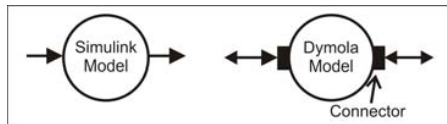


Fig. 5. Directed signal flow model of Matlab® / Simulink® in contrast to physical model based potential-flow models of Dymola® (quadrupoles)

model integration algorithms proposed for stiff systems were applied, since the standard integration algorithm did not work.

### III. RESULTS AND DISCUSSION

The cardiovascular model by Leaning et al. [2] and the heart model by Smith et al. [3], [4] were separately implemented and simulated. In the paper by Leaning et al. [2] no simulation results are given but, simulation results achieved with the basic heart model can be compared and validated with the publication by Smith et al. [3], [4].

Therefore, at first the simulation results for each model are presented and discussed. Since the left ventricular and the aortic pressure are critical in heart patients they are used for this comparison. In addition, a LVAD is typically connected to the left ventricular and ejects into the aorta ascendens which means that these pressure curves are of special interest. Furthermore, the stroke volumes for each model are illustrated since this is a critical parameter as well. Finally, few simulation results with the new model under normal and sick conditions are shown to prove the ability of the new model to simulate a patient with heart disease.

In Fig. 6 the pressures for the model by Leaning et al. [2] are depicted. The pressure for the left ventricular is between 1 mmHg and 140 mmHg which is a normal range. Values above 140 mmHg would not be acceptable, but the maximum value can be adjusted by changing the amplitude of the sine in the activation function. The characteristic for the aortic pressure curve corresponds to [12]. However, the pressure drop across the aortic valve is above 30 mmHg, even if it should be almost zero. This is emphasized by the ellipse plotted in Fig. 6. In this model the aortic valve is described by an inertance and two resistance terms, hence assumedly resistance values are too high. This problem might be solved by using other parameters for the resistances or adjusting the valve model itself. In Fig. 7 pressure curves achieved with the model by Smith et al. [3] are depicted. The change in the shape of the left ventricular curve is due to using a different activation function and can clearly be seen. As reported in [3], [4] the negative pressure with respect to atmospheric pressure of the left ventricular is noticeable (encircled in Fig. 7). The characteristic of the aortic curve in Fig. 7 differs from the curve in Fig. 6. In this model the pressure drop across the aortic valve is ca. 10 mmHg which matches better with physiological data. On the other hand, it is not possible to see the dicrotic notch in the pressure curve of the aortic valve (highlighted by the ellipse in Fig. 7). The dicrotic notch shows the transition from the systole to the diastole, hence, it marks the closure of the aortic valve. It can only be seen in vessels that are close to the heart. In this model, all arteries of

the systemic circulation are combined. Therefore, they have a higher damping ratio, making it impossible to see the dicrotic notch.

Simulation results for the the left ventricular and aortic pressure of the new model are shown in Fig. 8. In contrast to the left ventricular pressure curve from the model by [3] this one shows only positive values, which is achieved by the offset  $D_i$  in the activation function (see eq. 10). Due to the combination of the heart model with the more complex model of the vascular system the dicrotic notch can also be seen in the aortic pressure curve. Since the pressure drop across the valve in the model by Leaning et al. [2] was too high, the aortic valve proposed by [3] was used. In addition, the resistances of the valves were adapted leading to an even smaller pressure drop across the aortic valve and thus, delivering better results in comparison with [12]. Both effects are indicated by the ellipse in Fig. 8.

Fig. 9 shows the simulated stroke volume with each of the models. For the model proposed by Leaning et al. [2] the stroke volume is 58 ml at a heart frequency of 72 bpm (controlled by the arterial baroreceptorreflex). Therefore, the cardiac output is 4.18 l/min, which is slightly reduced and might be due to the provided elevated systemic resistance of the model. In the model by Smith et al. [3], [4] the stroke volume is about 70 ml which corresponds to a cardiac output of 5.25 l/min for the constant heart rate of 75 bpm. The cardiac output of the new model results in 5.2 l/min at a stroke volume of 63 ml. In this new model resistances were completely recalculated not only to match a desired distribution of the compartments but also to correspond to the typically reported value of  $1PRU = 1 \frac{mmHg}{ml/s}$  [10].

Additionally, the curve of the stroke volume of the model by Leaning et al. [2] as well as of the new model has another characteristic. This is due to the booster pump function of the atrium (meaning the contraction of the atrium) and is pointed out in Fig. 9.

For clarity's sake Fig. 10 and Fig. 11 show simulation results only for the new model. Fig. 10 presents the inflow and the outflow of the left ventricle. As previously described (see section II-D), flows out of a system have a negative sign. An outflow of ca. 600 ml/s is a normal value (compare [12]). In echocardiography the inflow characteristic into the left ventricle is important since it gives information about the diastolic function of the left ventricle. The normal flow profile into the left ventricle consists of the E- and the A-wave (see Fig. 10), where the E-wave corresponds to early passive left ventricular filling, whereas the A-wave complies with the late active filling of the left ventricle. In healthy conditions the relationship of "E/A" is supposed to be between "1-1.5" [13]. In the new model this value is "1.11".

Finally, PV-loops for a normal person as well as a patient with a reduced contractility and a patient with increased systemic resistances were created. The shift of the PV-loop for both cases compared to a normal PV-loop can clearly be seen in Fig. 11. In case of a reduced contractility the PV-diagram moves to the right. The endsystolic pressure reduces and more blood volume remains in the ventricle at the end of the systole due to the reduced pumping ability of the ventricle.

A marginal drop in the stroke volume (8ml) can also be seen. This corresponds to values reported in literature, [15].

In contrast, Fig. 11 shows a narrowed and prolonged PV-loop for a patient with an increased systemic resistance. I. e. a significant reduction of stroke volume (20ml) can be observed while simultaneously an increase for the endsystolic pressure is apparent. These findings are also reported in [14].

#### IV. SUMMARY

In summary, the suitability of the approach to embed a sophisticated heart model in an extended model of the cardiovascular system could be shown. Minor modifications like applying another activation function and adding the atria were introduced to the heart model to gain a useful model for simulating interactions with a mechanical blood pump. In the cardiovascular model, several modifications were necessary like adjusting the resistance as well as the compliance values of the vessels. The model of the vascular system was extended to allow the simulation of arm exercise as well as leg exercise. In addition, the adjustments applied to the models show significant improvements in the simulation results. Furthermore, the new model also includes the pulse wave reflections of the cardiovascular system. The new model can accurately mimic pressures and flows that are close to the heart.

#### ACKNOWLEDGMENT

The authors gratefully acknowledge the support provided by the Ziel2.NRW Program funded by the State of North Rhine-Westphalia (Germany) and the European Union, as part of the European Fund for Regional Development. Additionally, the authors thank the German research foundation (DFG) for financial support within the project LE817 / 5-1.

#### REFERENCES

- [1] T. Weber, *Grundlagen: Zentraler Blutdruck, Pulswellenreflexionen, Pulswellengeschwindigkeit*, J Hyperton, vol. 14, No. 2, pp. 9-13, 2010.
- [2] M. S. Leaning, H. E. Pullen, E. R. Carson and L. Finkelstein, *Modelling a complex biological system: the human cardiovascular system I. Methodology and model description*, Transaction of the Institute of Measurement and Control, vol. 5, pp.71-86, 1983.
- [3] B. W. Smith, J. G. Chase, R. I. Nokes, G. M. Shaw and G. Wake, *Minimal haemodynamic system model including ventricular interaction and valve dynamics*, Medical Engineering & Physics, vol. 26, pp.131-139, 2004.
- [4] B. W. Smith, J. G. Chase, G. M. Shaw, R. I. Nokes, *Experimentally verified minimal cardiovascular system model for rapid diagnostic assistance*, Control Engineering Practice, vol. 13, pp. 1183-1193, 2005.
- [5] J. E. W. Beneken and B. DeWit, *A physical approach to hemodynamic aspects of the human cardiovascular system*, Physical Bases of Circulatory Transport: Regulation and Exchange, E.B. Reeve and A. C. Guyton, W.B. Saunders Company, Philadelphia, 1967.
- [6] K. Lu, J. W. Clark, Jr., F. H. Ghorbel, D. L. Ware and A. Bidani, *A human cardiovascular model applied to the analysis of the Valsalva maneuver*, AAJP - Heart and Circulatory Physiology, vol. 281, pp. H2661-H2679, 2001.
- [7] R. Shabetai, L. Mangiardi, V. Bhargava, J. Ross, Jr., C. B. Higgins, *The Pericardium and Cardiac Function*, Progress in Cardiovascular Diseases, vol. XXII, No. 2, 107-134, 1979.
- [8] W. D. McArdle, F. I. Katch, V. L. Katch, *Exercise Physiology : Nutrition, Energy, and Human Performance*, 7th ed., Philadelphia, PA, USA: Lippincott Williams Wilkins, 2010.
- [9] M. F. Snyder, V. C. Rideout, R. J. Hillestad, *Computer modeling of the human systemic arterial tree*, J Biomech, vol. 1, pp. 341-353, 1968.
- [10] A. C. Guyton, J. E. Hall, *Textbook of medical physiology*, 11th. ed., Philadelphia, PA, USA: Elsevier Inc., 2006.
- [11] P. Fritzson, *Principles of Object-Oriented Modeling and Simulation with Modelica 2.1*, IEEE press, Piscataway, NJ; 2004.
- [12] S. Silbermagl, A. Despopoulos, *Taschenatlas Physiologie*, 7th. ed., Stuttgart, Germany, Thieme Verlag, 2007.
- [13] V. Hombach (Hrsg.), *Kardiovaskulaere Magnetresonanztomographie, Grundlagen-Technik-klinische Anwendung*, Stuttgart, Germany, Schattauer, 2005.
- [14] D. Burkhoff, I. Mirsky, H. Suga, *Assessment of systolic and diastolic ventricular properties via pressure-volume analysis: a guide for clinical, translational, and basic researchers*, Am J Physiol Heart Circ Physiol, vol. 289, pp.H501-H512, 2005.
- [15] H. Senzaki, C.-H. Chen, D. A. Kass, *Single-Beat Estimation of End-Systolic Pressure-Volume Relation in Humans, A New Method With the Potential for Noninvasive Application*, Circulation, vol. 94, pp.2497-2506, 1996.

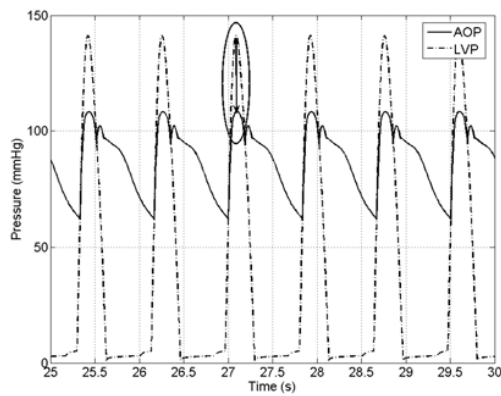


Fig. 6. Left Ventricular (LVP) and Aortic Pressure (AOP) simulated with the model by Leaning et al. [2]

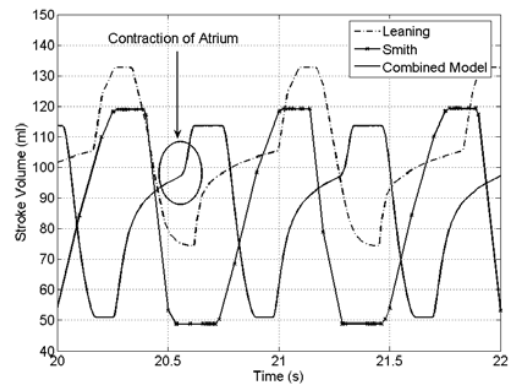


Fig. 9. Stroke Volume simulated with the Leaning, Smith and new model

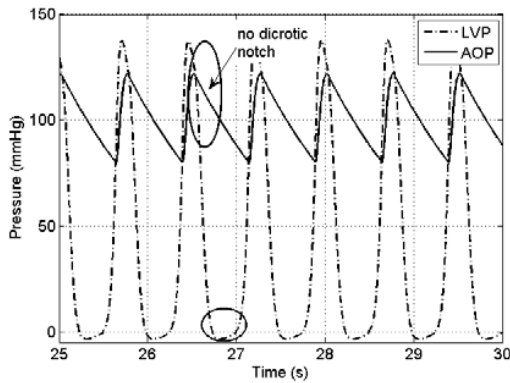


Fig. 7. Left Ventricular (LVP) and Aortic Pressure (AOP) simulated with the model by Smith et al. [3]

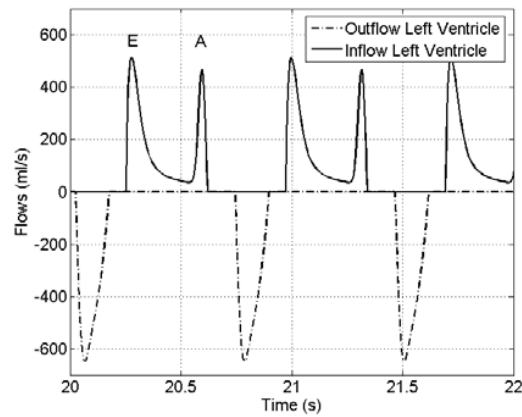


Fig. 10. Flows into and out of the Left Ventricle simulated with the new model

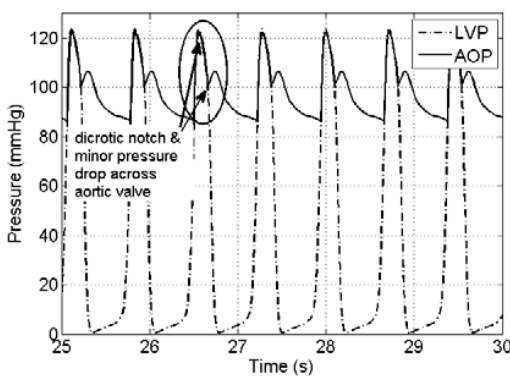


Fig. 8. Left Ventricular (LVP) and Aortic Pressure (AOP) simulated with the new model

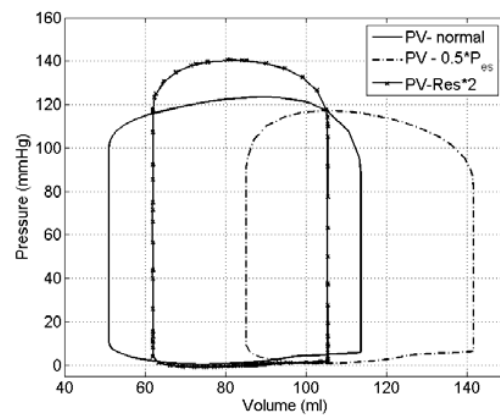


Fig. 11. PV-loops for a person with: normal values ( $PV - normal$ ), decreased contractility ( $PV - 0.5 * P_{es}$ ) & increased systemic resistance ( $PV - Res * 2$ ) simulated with the new model